JOURNAL OF
GENERAL VIROLOGY

RESEARCH ARTICLE
Herod *et al.*, *Journal of General Virology*
DOI 10.1099/jgv.0.001283

MICROBIOLOGY SOCIETY

The broad-spectrum antiviral drug arbidol inhibits foot-and-mouth disease virus genome replication

Morgan R. Herod[1], Oluwapelumi O. Adeyemi[1,2], Joseph Ward[1], Kirsten Bentley[3], Mark Harris[1], Nicola J. Stonehouse[1] and Stephen J. Polyak[4,5,*]

Abstract

Arbidol (ARB, also known as umifenovir) is used clinically in several countries as an anti-influenza virus drug. ARB inhibits multiple enveloped viruses *in vitro* and the primary mode of action is inhibition of virus entry and/or fusion of viral membranes with intracellular endosomal membranes. ARB is also an effective inhibitor of non-enveloped poliovirus types 1 and 3. In the current report, we evaluate the antiviral potential of ARB against another picornavirus, foot-and-mouth disease virus (FMDV), a member of the genus *Aphthovirus* and an important veterinary pathogen. ARB inhibits the replication of FMDV RNA sub-genomic replicons. ARB inhibition of FMDV RNA replication is not a result of generalized inhibition of cellular uptake of cargo, such as transfected DNA, and ARB can be added to cells up to 3 h post-transfection of FMDV RNA replicons and still inhibit FMDV replication. ARB prevents the recovery of FMDV replication upon withdrawal of the replication inhibitor guanidine hydrochloride (GuHCl). Although restoration of FMDV replication is known to require *de novo* protein synthesis upon GuHCl removal, ARB does not suppress cellular translation or FMDV internal ribosome entry site (IRES)-driven translation. ARB also inhibits infection with the related *Aphthovirus,* equine rhinitis A virus (ERAV). Collectively, the data demonstrate that ARB can inhibit some non-enveloped picornaviruses. The data are consistent with inhibition of picornavirus genome replication, possibly via the disruption of intracellular membranes on which replication complexes are located.

INTRODUCTION

The positive-sense RNA viruses of the family *Picornaviridae* include numerous important human and animal pathogens [1]. The family is divided into over 40 genera, including the genus *Aphthovirus,* which is composed of four species: bovine rhinitis A virus, bovine rhinitis B virus, equine rhinitis A virus and foot-and-mouth disease virus (FMDV) [1]. Whereas the first three of these species are of little medical or veterinary importance, FMDV is the causative agent of foot-and-mouth disease: a highly contagious, systemic infection of domestic and wild cloven-hooved ruminants [2]. The virus is endemic to many parts of the world, resulting in significant reductions in productive yields [3]. In disease-free countries, outbreaks in the population of domestic livestock result in the culling of millions of animals and significant economic losses. Major outbreaks in recent years have included the 2001 outbreak in the UK, which resulted in economic losses estimated at £8 billion [4, 5]. Although vaccines are available, control of the disease is limited by several factors. These include multiple virus serotypes and subtypes, the difficulty in distinguishing vaccinated from infected animals and an asymptomatic carrier state that some animals can develop [5, 6].

Picornaviruses are single-strand, positive-sense RNA viruses, with genomes ranging in size from 7 to 9 kilobases. The viral genome lacks a 5′ methylguanosine cap but instead contains a virion protein (VPg) that is covalently linked to the genome. At both the 5′ and the 3′ ends of the genome, there are untranslated regions (UTRs). The 5′UTR serves

Received 07 March 2019; Accepted 16 May 2019; Published 04 June 2019
Author affiliations: [1]School of Molecular and Cellular Biology, Faculty of Biological Sciences and Astbury Centre for Structural Molecular Biology, University of Leeds, Leeds, UK; [2]Current Address: Department of Medical Microbiology and Parasitology, Faculty of Basic Medical Sciences, College of Health Sciences, University of Ilorin, Ilorin, Nigeria; [3]School of Biology, University of St Andrews, St Andrews, UK; [4]Department of Laboratory Medicine, University of Washington, Seattle, WA, USA; [5]Department of Global Health, University of Washington, Seattle, WA, USA.
***Correspondence:** Stephen J. Polyak, polyak@uw.edu
Keywords: arbidol; antiviral; indole; FMDV; ERAV; picornavirus.
Abbreviations: ARB, arbidol; BSL2, biological safety level 2; CHX, cycloheximide; ERAV, equine rhinitis associated virus; FMDV, foot-and-mouth-disease virus; GFP, green fluorescent protein; GuHCl, guanidine hydrochloride; h, hour; IRES, internal ribosome entry site; μM, micromolar; ng, nanogram; ORF, open reading frame; p.f.u., plaque forming unit; RNA, ribonucleic acid; $TCID_{50}$, tissue culture infectious dose 50 %; UTR, untranslated region.

to initiate viral protein translation from a highly structured element called the internal ribosome entry site (IRES), while the 3′UTR plays a role in replication [1]. Between the 5′UTR and 3′UTR lies the coding region for the viral proteins that are expressed as a polyprotein. For FMDV, the order of viral proteins (encoded from 5′ to 3′) is L^{pol} protease, followed by P1 viral capsid proteins 1A, 1B, 1C, 1D [1]. Encoded next are the P2 viral non-structural proteins 2A, 2B and 2C with functions in genome replication, followed by P3 proteins comprising 3A, $3B_{1-3}$ and $3C^{pro}$ protease, and $3D^{pol}$ protein, which encodes the RNA-dependent RNA polymerase [1]. Individual viral proteins are generated by cleavage of the polyprotein by virally encoded proteases. All picornaviruses encode the viral protein $3C^{pro}$, while FMDV encodes an additional protease, L^{pro}, which cleaves itself from VP4 at the 5′ end of the genome [1]. In this study, we used FMDV replicons where the P1 viral structural proteins 1A, 1B, 1C and 1D were replaced with a *Ptilosarcus gurneyi* (sea pansy) GFP (ptGFP) open reading frame (ORF). When transfected into mammalian cells, *in vitro*-transcribed RNAs from this construct are replication-competent and produce high-level GFP expression, thereby facilitating studies on FMDV replication under Biological Safety Level 2 (BSL2) containment [7, 8].

The replication of most positive-sense RNA viruses occurs within, or on, cytoplasmic membrane-associated compartments. In the case of picornaviruses, these compartments must contain viral non-structural proteins including the viral RNA-dependent RNA polymerase ($3D^{POL}$), and primer for replication (known as 3B), along with host cell factors [1]. In co-localizing these components, the compartments are thought to provide a favourable environment for the synthesis of new viral genomes from the template positive strand via a negative strand intermediate. Generation of these replication compartments or 'factories' requires the subversion of host cell membranes that are derived from several host cell organelles [9]. Preventing the formation of such complexes would be an attractive target for the development of anti-viral therapeutics with a potentially broad action.

Arbidol (ARB, also known as umifenovir; PubChem CID 131410; Fig. 1), is a synthetic antiviral drug developed over 30 years ago to combat seasonal influenza virus [10]. ARB has been shown to inhibit viruses from many different families, including *Orthomyxoviridae* [11], *Paramyxoviridae* [12], *Bunyaviridae* [13], *Rhabdoviridae* [14], *Togaviridae* [15], *Hepadnaviridae* [16], *Hepaciviridae* [10, 17–20], *Filoviridae* [21], *Arenaviridae* [21, 22] and *Flaviviridae* [23, 24]. While all of these are enveloped viruses, ARB also inhibits non-enveloped viruses such as members of the *Picornaviridae*; specifically, poliovirus types 1 [25] and 3 (PV-1 and 3) [21]. In the current study, we evaluate the antiviral potential of ARB against FMDV, a picornavirus that causes widespread disease in animals.

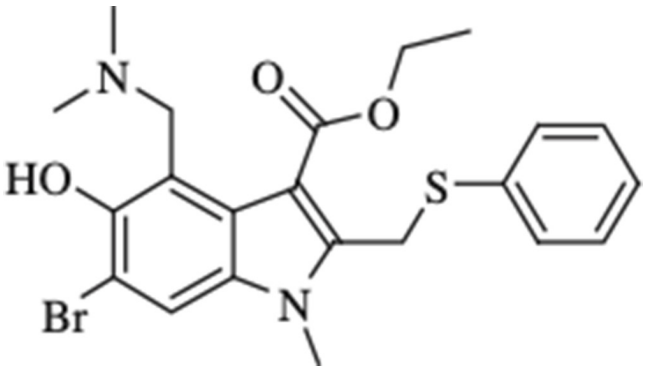

Fig. 1. Structure of arbidol (ARB).

RESULTS

FMDV sub-genomic replicons are a useful tool to study virus replication and antiviral efficacy under BSL2 containment. Replication can be assessed by the expression of a GFP reporter gene, by comparison to a replication-defective construct, which indicates the level of input translation. As a positive control, we used guanidine hydrochloride (GuHCl), a known inhibitor of picornavirus replication [26–29]. As expected, GuHCl abolished the replication of an FMDV replicon ($P<0.001$; Fig. 2). ARB (Fig. 1) treatment resulted in a dose-dependent suppression of FMDV replication, assessed as GFP fluorescence measured using an IncuCyte imaging system (Fig. 2, $P<0.001$). Doses of ARB of 9.4 μM and higher caused significant inhibition of FMDV replication ($P=0.035$ and lower). Non-linear regression analysis suggested that the concentration of ARB that caused 50 % suppression of FMDV replication (IC_{50}) ranged from 7 to 8.7 μM between 4 to 10 h post-transfection. Although not achieving statistical significance ($P=0.2$), even the lowest dose of ARB tested (1.88 μM) caused visible reduction in GFP expression (i.e. 40–48 % inhibition, Fig. 2b).

While GuHCl is a potent inhibitor of picornavirus replication, the effect is reversible [26]. GuHCl also caused potent suppression of FMDV replication ($P<0.0001$), and removal of GuHCl at 4 h post-transfection of FMDV RNA led to a rapid recovery in FMDV replication (Fig. 3a, b). Since ARB has been shown to block an early step in the infection of cells by many viruses [10, 17–23, 30], we performed a time-of-addition experiment to define the latest time at which ARB could be added to replicon-transfected cells and still inhibit FMDV replication. Fig. 3c shows that ARB can be added up to 3 h post-transfection and still cause significant inhibition of FMDV replication. Although adding ARB at 4 h post-transfection caused inhibition of FMDV replication, the effect did not always achieve statistical significance (see below). We next examined the effect of ARB and GuHCl on FMDV replication, choosing 4 h post-transfection as the time to compare the effect of ARB addition and GuHCl removal. As in Fig. 2, both ARB and GuHCl inhibited FMDV replication when added to cells just before transfection (Fig. 3d red and green bars, $P<0.001$). ARB inhibited replicon replication when added 4 h post-transfection, albeit less efficiently (Fig. 3D, purple

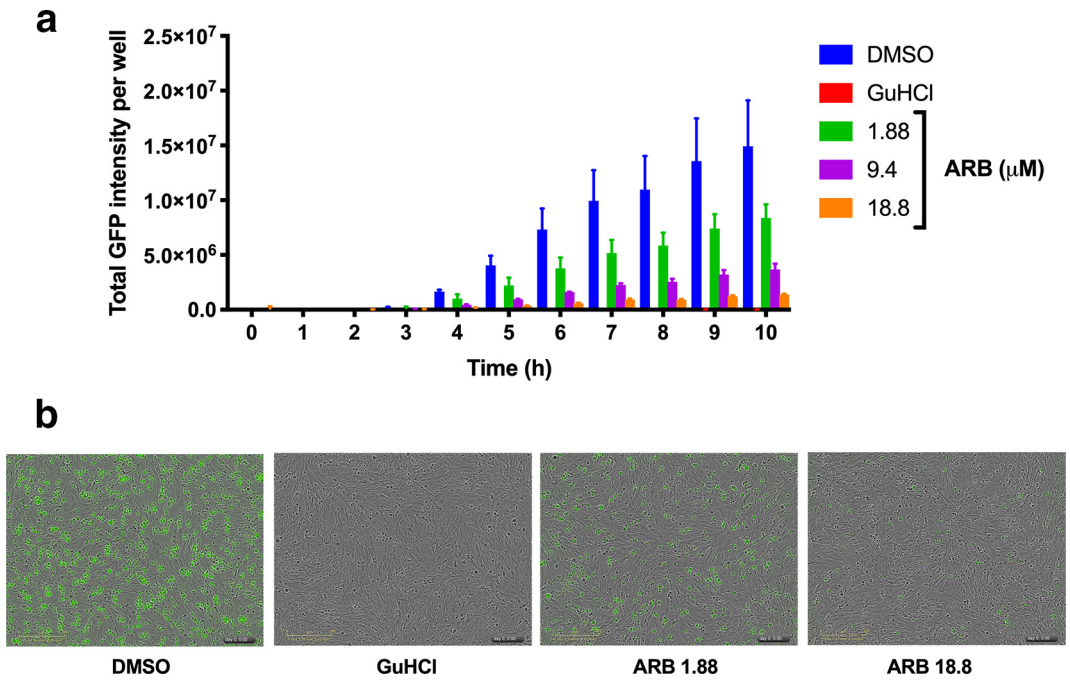

Fig. 2. ARB inhibits FMDV replication. BHK-21 cells treated with DMSO, 2 mM guanidine hydrochloride (GuHCl), or the indicated doses of ARB were immediately transfected with wild-type GFP FMDV replicon. (a) FMDV replication was monitored by total GFP expression at hourly intervals over 10 h. Absolute values for total GFP intensity per well from a representative experiment of two independent repeats are shown. The data depict the means and standard deviations of duplicate measurements for each condition. (b) Representative images of total cells and GFP-positive cells from the 8 h timepoint.

bars, P=0.015) as compared to when it was added at the start of the experiment. When GuHCl was removed at 4 h post-transfection, FMDV replication was reactivated (Fig. 3d, orange bars, P<0.001). ARB, when added to cells from the start of the experiment, inhibited the resumption of FMDV replication when GuHCl was removed (Fig. 3d, black bars, P<0.001). Delaying the addition of ARB to cells until 4 h post-transfection also inhibited the resumption of FMDV replication upon GuHCl removal, but the inhibition was less effective as compared to when ARB was added to cells at the start of the experiment (data now shown). These data suggest that ARB is maximally effective in suppressing FMDV replication when added to cells before and within the first 3 h of transfection of FMDV RNA replicons, and that ARB can inhibit the recovery of FMDV replication upon GuHCl withdrawal. ARB had minimal effects on basal GFP levels expressed from replication-defective FMDV replicons that contained a mutation in the FMDV RNA polymerase active site (GNN; data not shown). The data suggest that ARB directly inhibits FMDV replication, does not affect transfection of the RNA replicon itself, and does not affect translation from input FMDV RNA templates (see below).

Because ARB did not significantly inhibit FMDV replication when added 4 h post-transfection of FMDV RNA replicons, and because ARB can block the entry of many enveloped viruses [10, 21–23], we asked whether ARB could inhibit the transfection that is required to initiate FMDV replicon replication. For this, we tested the ability of ARB to inhibit GFP expression following plasmid DNA transfection. When ARB was only incubated with cells during the 4 h transfection, there was no effect on GFP expression when analysed microscopically (Fig. 4b) or by Western blot (Fig. 4c, d). The data indicate that ARB does not affect the uptake of cargo such as plasmid DNA.

Resumption of picornavirus replication upon the removal of GuHCl requires *de novo* protein synthesis [29]. Since ARB inhibits the recovery of FMDV replication upon GuHCl withdrawal, we hypothesized that ARB might be inhibiting translation. More specifically, we posited that ARB inhibits FMDV translation, which is initiated in a cap-independent fashion by an IRES, a feature in the 5′ UTRs of many positive-strand RNA viruses, including FMDV [31, 32]. To test the hypothesis, we utilized a plasmid, pRF-FMDV, which produces a bicistronic RNA containing two ORFs for two different luciferase reporters. The first ORF expresses *Renilla* luciferase by cellular cap-dependent translation (and can also initiate translation from non-capped RNAs [33]), while the second ORF expresses firefly luciferase from the FMDV IRES (Fig. 5a) [34, 35]. When the pRF-FMDV plasmid DNA was transfected into Huh7.5.1 cells, the translation inhibitor cycloheximide (CHX) suppressed both *Renilla* and firefly luciferase levels, indicating suppression of translation (Fig. 5b). Removal of CHX relieved the suppression of translation, resulting in strong induction of translation from both reporters, and

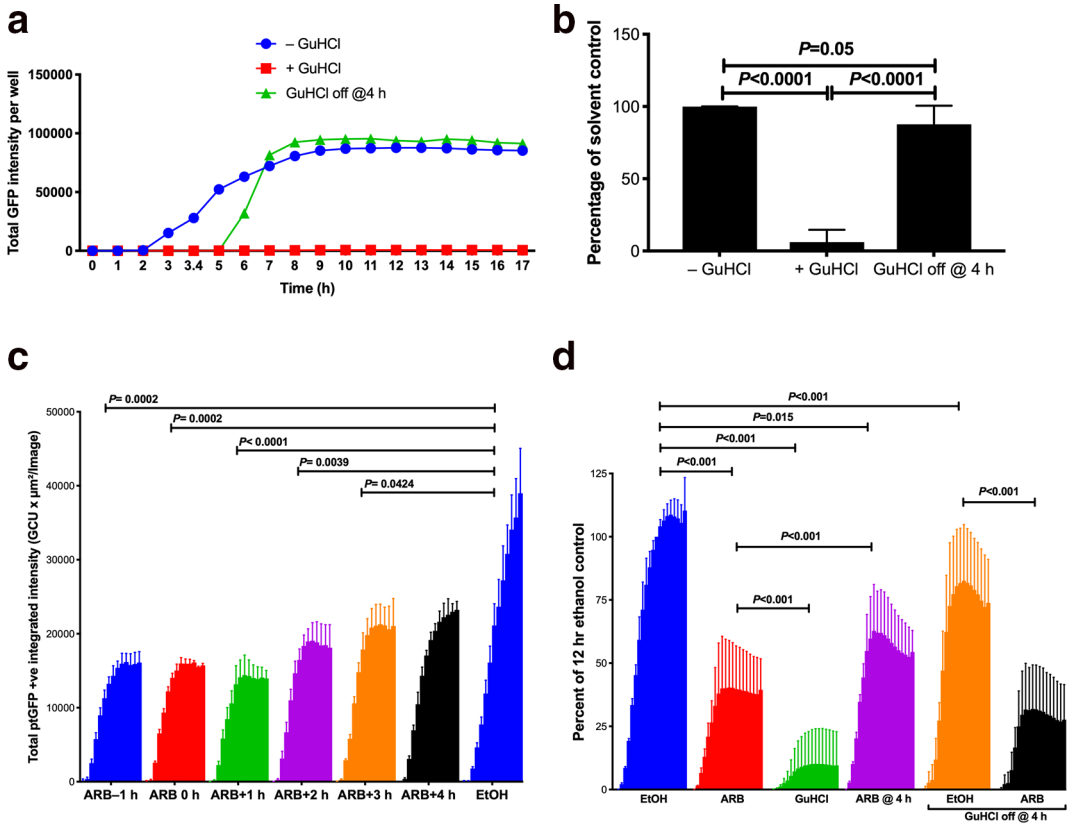

Fig. 3. ARB inhibits recovery of FMDV replication after GuHCl withdrawal. (a) GuHCl reversibly inhibits FMDV replication. BHK-21 cells were transfected with wild-type GFP FMDV replicon and immediately treated with DMSO or DMSO plus 2 mM GuHCl. GuHCl was either left on for the duration of the experiment (GuHCl left on) or removed at 4 h post-transfection (p.t.; GuHCl removed 4 h p.t.) and replaced with normal media. FMDV replication was monitored by total GFP expression at hourly intervals over 17 h. The data are representative of an experiment that was performed five times: pooled data from the five replicates are shown in (b), where *P* values were derived from one-tailed *t*-tests in Excel, with the comparison groups connected via the indicated lines. (c) BHK-21 cells were treated at the indicated times with 10 µM ARB (or ethanol solvent control, EtOH) in the context of transfection with the FMDV RNA that expresses HA-tagged 3A and Flag-tagged 3D proteins. FMDV replication was monitored by total GFP expression at hourly intervals over 14 h. The data are derived from a single experiment. (d) BHK-21 cells were transfected with the FMDV replicon containing HA-tagged 3A and Flag-tagged 3D RNA replicon. Just prior to addition of transfection complexes, media containing the following compounds were added to separate wells of cells: 0.1 % ethanol (EtOH, blue bars), 10 µM ARB (ARB, red bars), 2 mM GuHCl (green bars). Separately, ARB was added 4 h post-transfection (ARB @4 h, purple bars). GuHCl was also removed at 4 h post-transfection (GuHCl off @4 h) and replaced with media containing 0.1 % ethanol (EtOH, orange bars) or 10 µM ARB (black bars). In the GuHCl removal arm, both EtOH and ARB were added with GuHCl at the start of the experiment. FMDV replication was monitored by total GFP expression at hourly intervals over 12 h. The data depict the means and standard deviations of three separate experiments, with all conditions in triplicate. *P* values for panels (c) and (d) were derived from one-way ANOVA tests in GraphPad Prism, with the comparison groups connected via the indicated lines.

ARB treatment had minimal effects on translation from both reporters (Fig. 5b). To reinforce these data, we generated bicistronic RNA from the pRF-FMDV plasmid by *in vitro* transcription. We did not add 5′ methylguanosine caps to these RNA transcripts, as we have previously shown that non-capped RNAs are efficiently translated [33], presumably due to the high level of RNA in the cytoplasm following transfection, which leads to translational initiation by ribosome scanning, as previously demonstrated for non-capped mRNAs [36]. As expected, CHX treatment reduced the expression of both *Renilla* and firefly luciferases (Fig. 5c). Although ARB showed some reduction of FMDV-IRES-driven firefly luciferase, ARB caused a more pronounced, dose-dependent suppression of cell viability (Fig. 5c). Taken together, these data indicate that ARB does not suppress translation.

Due to stringent regulations that restrict work with infectious FMDV, it was not possible to extrapolate our FMDV replicon data to determine the effect of ARB on FMDV infection. As an alternative approach to validate the FMDV replicon data we therefore tested ARB against equine rhinitis A virus (ERAV), a picornavirus in the same genus as FMDV (*Aphthovirus*). Unlike FMDV, ERAV can be propagated in a standard BSL2 containment laboratory. ARB was added to overlay media in both plaque and $TCID_{50}$ ERAV titration assays after a

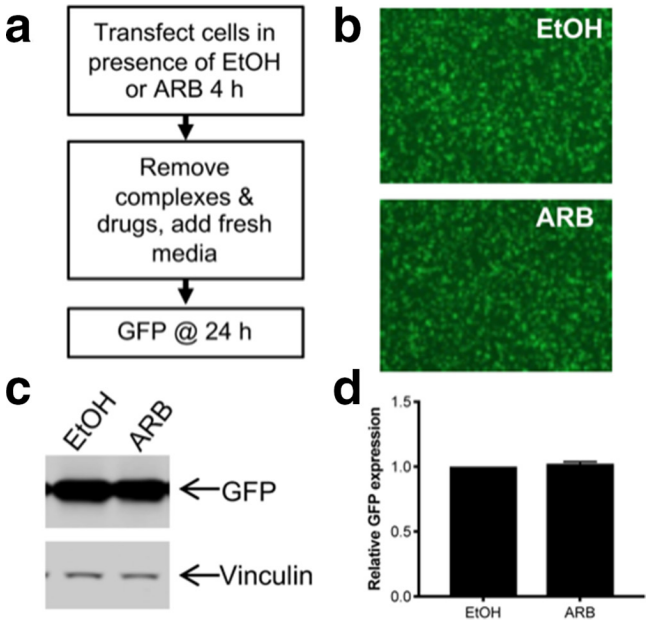

Fig. 4. ARB does not block uptake of plasmid DNA. (a) Schematic of experiment. Huh7.5.1 cells were transfected with pEGFP plasmid using X-tremeGENE 9 DNA Transfection Reagent. Cells were incubated with DNA–transfection cocktail for 4 h in the presence of ethanol solvent control (EtOH) or 18.8 µM of ARB in ethanol. The inocula were removed, the cells were washed and fresh medium (without EtOH or ARB) was added to the cells. GFP was measured at 24 h post-transfection. (b) Representative EVOSfl microscopy images of EtOH- versus ARB-treated cells. (c) Representative Western blot of GFP and vinculin (a cellular protein control) in EtOH- versus ARB-treated cells. (d) Band intensity analysis of the cells that were treated with EtOH or ARB for 4 h during transfection. The data are derived from three independent experiments and represent the averages and standard deviations of GFP pixel intensities normalized to cellular vinculin levels.

1 h adsorption of virus to cells. Fig. 6 shows that ARB caused dose-dependent inhibition of ERAV in both titration assays with an IC_{50} of approximately 4–5 µM.

DISCUSSION

In addition to the clear antiviral effects of ARB that suppress the entry of enveloped viruses, specifically fusion [10, 17–22, 30], ARB also inhibits the infection of cells by non-enveloped picornaviruses, including PV-1 [25] and PV-3 [21] while, as shown in this report, it inhibits FMDV replication and ERAV infection. We know that ARB can inhibit enveloped viruses by blocking post-entry events because of studies showing that ARB inhibits non-infectious HCV replicons [18], while the drug can inhibit Ebola virus and Zika virus when added up to 24 h post-infection [21, 23]. Although the ability of ARB to suppress virus replication when added after infection is not as great compared to when cells are treated with ARB before or within a few hours of infection, collectively these studies indicate that ARB inhibits virus replication.

A major question for future work is how ARB blocks FMDV replication and how it prevents the resumption of FMDV replication upon GuHCl removal. ARB is known to engage membranes [19, 20], so this activity should be considered as a potential mechanism for the suppression of FMDV replication. This indole-based hydrophobic molecule displays dual binding capacity to both lipid membrane interfaces and to aromatic protein residues and viral proteins that are embedded in membranes [20, 30]. Thus, ARB might also impair virus replication on intracellular membranes which are remodelled during the replication of many positive-strand viruses, including picornaviruses [9, 37]. Previous studies with GuHCl to stall poliovirus replication showed that GuHCl does not inhibit the synthesis or processing of viral proteins [27], yet *de novo* protein synthesis and cellular factors are required to resume replication upon GuHCl removal [27, 29]. Moreover, GuHCl blocks negative-strand synthesis in cell-free systems [28], possibly through inhibition of the viral 2C protein, which is a membrane-associated component of the viral RNA replication complex [38, 39]. Indeed, GuHCl-resistant mutants map to the 2C protein for several picornaviruses, including FMDV [29, 40]. Since ARB did not inhibit translation, we can rule out inhibition of *de novo* protein synthesis as the mechanism of action for ARB suppression of resumption of FMDV replication upon GuHCl removal. Instead, ARB showed maximal inhibition of FMDV replication when cells were treated 1 h before, and up to 3 h after, the transfection of FMDV RNA replicons. If ARB requires time to impregnate intracellular membranes, then it might disrupt the interactions of nascent viral replication complex proteins with membranes. Disruption of protein–protein interactions during replication complex formation is also possible, given the propensity of ARB to engage membranes, proteins in membranes and protein conformational changes [20, 30]. However, since ARB can still suppress FMDV replication when added up to 3 h post-transfection of FMDV RNA replicons, and ARB does not inhibit cellular or IRES-mediated translation, it is not likely to inhibit early replication events, such as polyprotein expression and proteolytic processing. The fact that ARB can be added up to 3 h post-infection suggests that it is also not inhibiting either positive- or negative-strand RNA synthesis, as both of these processes occur within the first 3 h of picornavirus infection [41]. Furthermore, during poliovirus infection, the intracellular location of viral proteins and positive- and negative-strand RNA changes over time. Within the first 2.5 h of infection, input positive-strand RNA and the viral 2B protein are translated on the endoplasmic reticulum, producing a diffuse cytoplasmic staining pattern, which correlates with the formation of virus-induced intracellular vesicles [41], a hallmark of intracellular membrane rearrangement associated with poliovirus infection [42]. By 3.5 h of infection, viral RNAs, the 2B protein and vesicles move closer to the nucleus, generating a punctate perinuclear staining pattern [41]. This movement is dependent on microtubules, since the migration can be inhibited with nocodazole [41]. Moreover, GuHCl causes viral 2B protein and positive-strand RNA to become concentrated as large juxtanuclear dots associated with the Golgi apparatus [41].

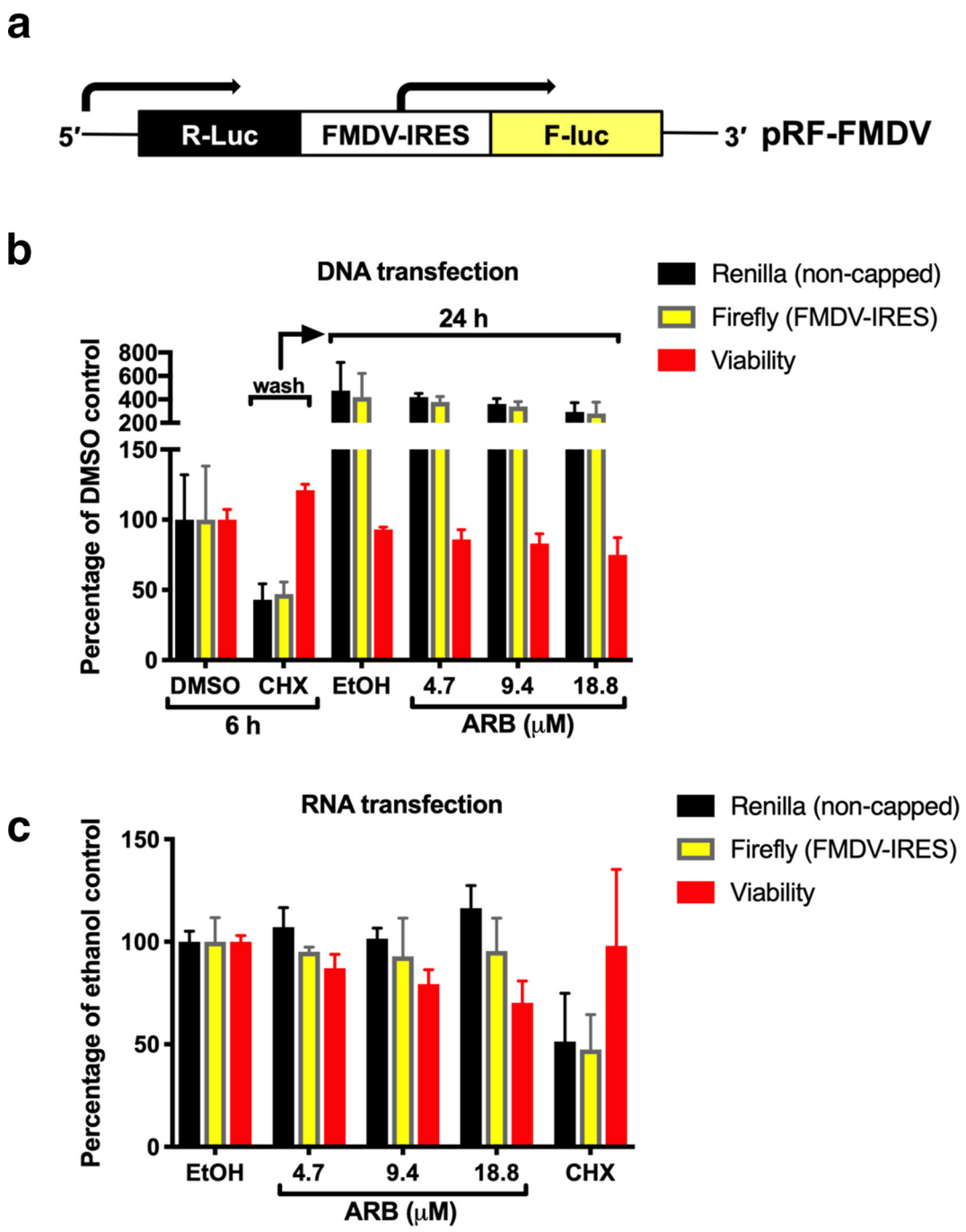

Fig. 5. ARB does not inhibit translation. (a) Schematic of bicistronic reporter gene plasmid, pRF-FMDV, showing the translation of *Renilla* luciferase (R-luc) regulated by standard cellular translation, whereas firefly luciferase (F-luc) is translated from the FMDV internal ribosome entry site (IRES). (b) pRF-FMDV plasmid DNA was transfected into Huh7.5.1 hepatoma cells and 18 h later cells were treated with DMSO or 10 µg ml^{-1} cycloheximide (CHX) for 6 h. CHX-treated cells were then washed and medium containing ethanol solvent control (EtOH) or the indicated doses of ARB solubilized in EtOH was added to cells. *Renilla* and firefly luciferase activity was measured 24 h later by DualGlo assay. Viability was measured in parallel wells by measuring ATP levels via ATPlite assay. The data shown are normalized to the 6 h DMSO control and represent the means and standard deviations of triplicate samples per condition. The experiment was performed once. (c) Ethanol (EtOH), the indicated doses of ARB solubilized in EtOH, or CHX was added to Huh7 cells immediately before lipofectin-based transfection of 50 ng of *in vitro*-transcribed RNA from pRF-FMDV. *Renilla* and firefly luciferase activity was measured 17 h later by DualGlo assay. Cell viability was measured via ATPlite assay. The experiment was performed twice and the data represent pooled data with each condition in each experiment performed in triplicate.

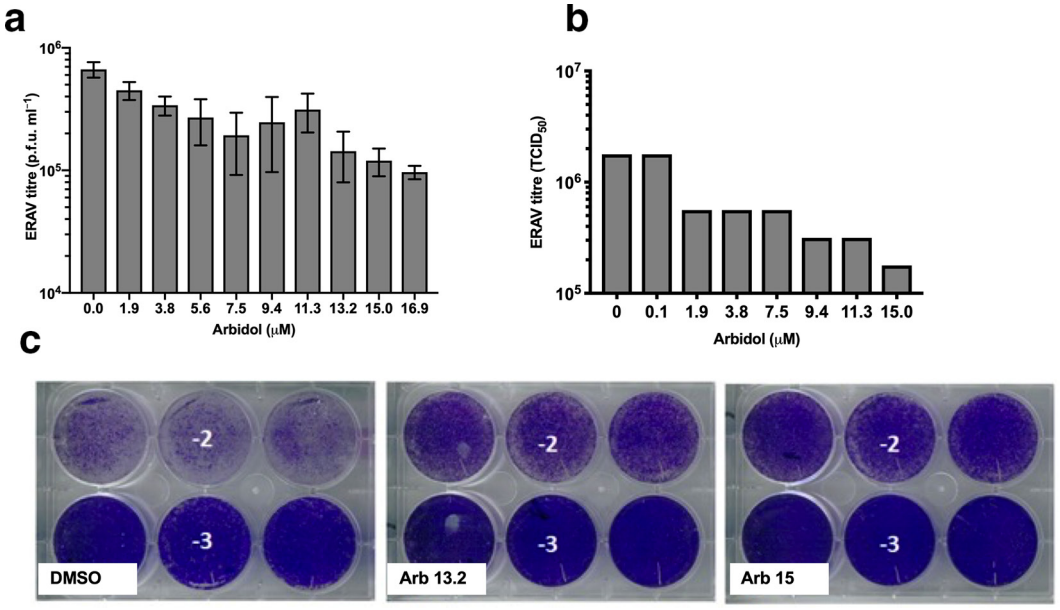

Fig. 6. ARB inhibits ERAV infection. (a) BHK-21 cells were infected with serial 1 : 10 dilutions of ERAV virus stock for 1 h at 37 ˚C. Virus inocula were removed and cells were overlaid with overlay media containing the indicated doses of ARB. Plaques were stained with crystal violet 96 h post-infection. Plaques were counted and titres were calculated as described in the Methods section. (b) BHK-21 cells were infected with serial 1 : 10 dilutions of ERAV virus stock for 1 h at 37 ˚C. Virus inocula were removed and cells were overlaid with fresh media containing the indicated μM doses of ARB. Cells were stained with crystal violet 72 h later. The $TCID_{50}$ was calculated as described in the the Methods section. (c) Representative titre plates from the data shown in (a) (−2 and −3 refer to serial 1 : 100 and 1 : 1000 dilutions of ERAV-containing supernatants). The plaque assay and $TCID_{50}$ assay were each performed once.

Within 1 h of GuHCl removal, positive-strand RNA and 2B protein move from the large juxtanuclear dots back to the diffuse cytoplasmic ER staining pattern, and after 1.5 h of GuHCl release, positive- and negative-strand RNA and viral 2B protein re-establish their punctate perinuclear staining [41]. Thus, it is possible that the propensity of ARB to interact with proteins embedded in membranes and membranes themselves could influence the trafficking and/or integrity of replication complexes on intracellular membranes that are required to resume FMDV replication upon GuHCl removal. These hypotheses merit further study.

ARB has been used clinically for decades in several countries, with minimal side-effects and a good pharmacokinetic profile [10, 17, 43]. Further studies on ARB in the context of FMDV infection, replication and in small animal models are required to determine whether ARB has utility for prophylactic and therapeutic use in FMD outbreaks in animals.

METHODS

Starting material

ARB (Fig. 1) was synthesized commercially. Purity and structure were confirmed as described [21]. ARB was dissolved in ethanol or DMSO.

Cells

Huh7.5.1 (human hepatoma [44]), Huh7 (human hepatoma [45]), Vero (African green monkey kidney [46]), adherent HeLa Ohio (human epithelial carcinoma cells) and BHK-21 (baby hamster kidney cells) cells [47] were grown as described previously [48, 49].

FMDV replicons

The FMDV replicon plasmids, pRep-ptGFP, and the equivalent constructs containing the replication-defective 3D^{pol}-GNN point mutation to the RNA polymerase have already been described [8]. For some experiments, a GFP-expressing replicon construct containing HA-tagged 3A and Flag-tagged 3D proteins was also used. The insertion of either epitope tag does not affect replicon replication, as we have previously described [8, 50]. Replicon plasmid was linearized with *Asc*I (NEB) before use in T7 *in vitro* transcription reactions as previously described [8]. Replicon RNA was purified using an RNA Clean and Concentrator-25 kit (Zymo Research), following the manufacturer's instructions. Prior to transfection, transcripts were quantified and qualified by denaturing MOPS/formaldehyde gel following standard protocols.

Viruses

Viral stocks of equine rhinitis A virus (ERAV) [51] were generated by infecting HeLa Ohio cells at a multiplicity

of infection (m.o.i.) of 1. The resulting supernatants were harvested by low-speed centrifugation and titred on HeLa Ohio cells by standard plaque assay [52].

ARB treatment

ARB was added to cells before virus infection or FMDV RNA replicon transfection, except for in time-of-addition studies, where the drug was added before, during and after infection or transfection. Please refer to the figure legends for details of when ARB was added.

FMDV replication assay

BHK-21 cells seeded into 24-well tissue culture plates were allowed to adhere for 16 h before replicate wells were transfected with replicon transcripts at 500 ng RNA per well using Lipofectin reagent (Thermo Scientific) as previously described [49]. Arbidol was added directly to duplicate wells per concentration assayed at the indicated time points relative to transfection. Fluorescent reporter protein expression was monitored using an IncuCyte Zoom Dual Color FLR (Essen BioSciences) within a 37 °C humidified incubator. Wells were scanned hourly up to 24 h post-transfection and captured images were analysed using the associated software for fluorescent protein expression. The fluorescent thresholds for analysis were determined using control transfections and were used to identify fluorescent positive objects from background fluorescence, as described previously [49].

ERAV infection

The titres of ERAV were determined by plaque assay following standard procedures. Briefly, serial dilutions of virus or virus complexes were added to HeLa Ohio cell monolayers and incubated on a rocking platform for 60 min. The virus inoculum was removed and replaced by growth medium containing 1 % agarose (Lonza SeaKem LE) supplemented with arbidol at the indicated concentration. The plates were incubated for 96 h and fixed with 4 % paraformaldehyde, and plaques were visualized by crystal violet staining. For $TCID_{50}$ determinations, 96-well plates were seeded with 1×10^4 Vero cells per well in 100 µl of complete growth media and grown overnight. ERAV was serially diluted 1 : 10 from 10^{-1} to 10^{-7} in serum-free medium and 100 µl of each dilution was added to cells in triplicate. Serum-free medium alone was added as a negative control. Virus was adsorbed to cells for 2 h at 37 ˚C, after which it was removed and replaced with 100 µl of medium containing various concentrations of ARB. Cells were fixed in 4 % paraformaldehyde for 20 min before being stained with crystal violet. The $TCID_{50}$ was calculated using Reed–Muench method, using a freely available calculator [53].

Plasmid uptake assay

Huh7.5.1 cells were seeded in 12-well tissue culture plates at 200 000 cells per well. The next day, cells were transfected with 500 ng/well of pEGFPN1 plasmid (Clontech) using X-tremeGENE 9 DNA Transfection Reagent (Sigma Aldrich). Cells were incubated with DNA transfection cocktail for 4 h in the presence of ethanol solvent control (EtOH) or 18.8 µM of ARB in ethanol. The medium and drugs were removed, the cells were washed and fresh medium without drugs was added to the cells. GFP was measured at 24 h post-transfection, both by Western blot with anti-GFP antibodies (sc-9996, Santa Cruz Biotechnology) and by EVOS-FL fluorescence microscopy (Thermo Fisher). Western blots were imaged by the Odyssey imaging system (LI-COR). GFP levels were normalized against Western blot detection of the cellular protein vinculin (sc-73614, Santa Cruz Biotechnology). For all Western blots, Image Studio (LI-COR) software was used to obtain Western blot images, using the default instrument settings of resolution at 169 µm and scan quality set to lowest. Any image manipulations were manually applied equally across the entire image and were applied equally to controls. The manipulations consisted of adjusting the brightness and contrast and/or flipping the image to obtain the proper orientation. Using Image Studio software, rectangles of identical size and area were drawn around GFP and vinculin to obtain pixel intensities, which were exported into Excel. GFP levels were normalized to vinculin levels. ARB-treated samples were then normalized to the EtOH by dividing the normalized GFP intensity of ARB-treated cells by the normalized GFP intensity of ethanol-treated cells.

Translation assays

Bicistronic plasmid DNA was obtained from Kensuke Hirasawa (Memorial University). The plasmid contains two luciferase reporter genes: *Renilla* luciferase (R-luc) whose translation is 5′ methylguanosine cap-dependent, and firefly luciferase (F-luc), which is translated by an FMDV IRES [34]. Fifty nanograms of the bicistronic plasmid DNA was transfected into Huh7.5.1 hepatoma cells using X-tremeGENE 9 DNA Transfection Reagent (Sigma Aldrich), and 18 h later the cells were treated with DMSO or 10 µg ml^{-1} cycloheximide (CHX) for 6 h. CHX-treated cells were then washed and medium containing EtOH or the indicated doses of ARB solubilized in EtOH was added to the cells. *Renilla* and firefly luciferase activity was measured 24 h later by DualGlo assay (Promega). Viability was measured in parallel wells by measuring the ATP levels via ATPlite assay (Perkin Elmer).

In vitro transcription of bicistronic constructs

RNA was also generated from the pRF-FMDV plasmids using the RiboMax kit (Promega). Plasmids were linearized with *Bam*HI and run-off transcripts were made. For this study, we did not cap RNA transcripts from these plasmids, as we have previously shown that non-capped RNAs are translated [33] because of the high level of RNA in the cytoplasm following transfection, which leads to translational initiation by ribosome scanning [36]. Huh7 cells were treated with EtOH, ARB solubilized in EtOH, or with CHX immediately before 50 ng of RNA was transfected into Huh7 cells using Lipofectin (Invitrogen). *Renilla* and firefly luciferase activity was measured 17 h later by DualGlo assay (Promega).

Cytotoxicity testing

The cytotoxicity of ARB on Huh7.5.1 or Huh7 cells was evaluated by measuring cellular ATP levels with a commercial kit (ATPlite assay, Perkin Elmer) or by MTT assay. The cytotoxicity of ARB on BHK-21 cells was measured using MTS assay (Promega).

Statistics

Data were analysed by one-sided *t*-tests in Excel software or by one-way analysis of variance (ANOVA) using GraphPad Prism software.

Funding information
This research was partially supported by a Cheney Fellowship to S. J. P. from the University of Leeds. Support from BBSRC grant BB/P001459/1 to N. J. S. and BBSRC Studentship BB/F01614X/1 to J. W. is also gratefully acknowledged.

Acknowledgements
We thank Maria Licursi and Kensuke Hirasawa for bicistronic plasmid constructs. We also thank Jessica Wagoner, Natalie Jones, Danial Power, Josh Jarrett and Ethan Doherty for technical support. S. J. P. and M. H. thank Stark Polarris for helpful and lively discussions.

Conflicts of interest
The authors declare that there are no conflicts of interest.

References

1. Fields BN, Knipe DM, Howley PM. *Fields virology*, 6th ed. Philadelphia: Wolters Kluwer Health/Lippincott Williams & Wilkins; 2013.
2. Jamal SM, Belsham GJ. Foot-and-mouth disease: past, present and future. *Vet Res* 2013;44:116.
3. Souley Kouato B, De Clercq K, Abatih E, Dal Pozzo F, King DP *et al*. Review of epidemiological risk models for foot-and-mouth disease: implications for prevention strategies with a focus on Africa. *PLoS One* 2018;13:e0208296.
4. Thompson D, Muriel P, Russell D, Osborne P, Bromley A *et al*. Economic costs of the foot and mouth disease outbreak in the United Kingdom in 2001. *Rev Sci Tech* 2002;21:675–687.
5. Knight-Jones TJ, Rushton J. The economic impacts of foot and mouth disease – what are they, how big are they and where do they occur? *Prev Vet Med* 2013;112:161–173.
6. Alexandersen S, Zhang Z, Donaldson AI. Aspects of the persistence of foot-and-mouth disease virus in animals—the carrier problem. *Microbes Infect* 2002;4:1099–1110.
7. Tulloch F, Pathania U, Luke GA, Nicholson J, Stonehouse NJ *et al*. FMDV replicons encoding green fluorescent protein are replication competent. *J Virol Methods* 2014;209:35–40.
8. Herod MR, Loundras EA, Ward JC, Tulloch F, Rowlands DJ *et al*. Employing transposon mutagenesis to investigate foot-and-mouth disease virus replication. *J Gen Virol* 2015;96:3507–3518.
9. Romero-Brey I, Bartenschlager R. Membranous replication factories induced by plus-strand RNA viruses. *Viruses* 2014;6:2826–2857.
10. Blaising J, Polyak SJ, Pécheur EI. Arbidol as a broad-spectrum antiviral: an update. *Antiviral Res* 2014;107:84–94.
11. Leneva IA, Fediakina IT, Gus'kova TA, Glushkov RG. [Sensitivity of various influenza virus strains to arbidol. Influence of arbidol combination with different antiviral drugs on reproduction of influenza virus A]. *Ter Arkh* 2005;77:84–88.
12. Shi L, Xiong H, He J, Deng H, Li Q *et al*. Antiviral activity of arbidol against influenza A virus, respiratory syncytial virus, rhinovirus, coxsackie virus and adenovirus *in vitro* and *in vivo*. *Arch Virol* 2007;152:1447–1455.
13. Deng HY, Luo F, Shi LQ, Zhong Q, Liu YJ *et al*. Efficacy of arbidol on lethal hantaan virus infections in suckling mice and *in vitro*. *Acta Pharmacol Sin* 2009;30:1015–1024.
14. Blaising J, Lévy PL, Polyak SJ, Stanifer M, Boulant S *et al*. Arbidol inhibits viral entry by interfering with clathrin-dependent trafficking. *Antiviral Res* 2013;100:215–219.
15. Delogu I, Pastorino B, Baronti C, Nougairède A, Bonnet E *et al*. *In vitro* antiviral activity of arbidol against Chikungunya virus and characteristics of a selected resistant mutant. *Antiviral Res* 2011;90:99–107.
16. Zhao C, Zhao Y, Chai H, Gong P. Synthesis and *in vitro* anti-hepatitis B virus activities of some ethyl 5-hydroxy-1H-indole-3-carboxylates. *Bioorg Med Chem* 2006;14:2552–2558.
17. Boriskin YS, Leneva IA, Pecheur EI, Polyak SJ. Arbidol: a broad-spectrum antiviral compound that blocks viral fusion. *Curr Med Chem* 2008;15:997–1005.
18. Boriskin YS, Pécheur EI, Polyak SJ. Arbidol: a broad-spectrum antiviral that inhibits acute and chronic HCV infection. *Virol J* 2006;3:56.
19. Pécheur EI, Lavillette D, Alcaras F, Molle J, Boriskin YS *et al*. Biochemical mechanism of hepatitis C virus inhibition by the broad-spectrum antiviral arbidol. *Biochemistry* 2007;46:6050–6059.
20. Teissier E, Zandomeneghi G, Loquet A, Lavillette D, Lavergne JP *et al*. Mechanism of inhibition of enveloped virus membrane fusion by the antiviral drug arbidol. *PLoS One* 2011;6:e15874.
21. Pécheur EI, Borisevich V, Halfmann P, Morrey JD, Smee DF *et al*. The synthetic antiviral drug arbidol inhibits globally prevalent pathogenic viruses. *J Virol* 2016;90:3086–3092.
22. Hulseberg CE, Fénéant L, Szymańska-de Wijs KM, Kessler NP, Nelson EA *et al*. Arbidol and other low-molecular-weight drugs that inhibit Lassa and Ebola viruses. *J Virol*, in press 2019;93.
23. Fink SL, Vojtech L, Wagoner J, Slivinski NSJ, Jackson KJ *et al*. The antiviral drug arbidol inhibits Zika virus. *Sci Rep* 2018;8:8989.
24. Haviernik J, Štefánik M, Fojtíková M, Kali S, Tordo N *et al*. Arbidol (Umifenovir): a broad-spectrum antiviral drug that inhibits medically important arthropod-borne flaviviruses. *Viruses* 2018;10:184.
25. Brooks MJ, Burtseva EI, Ellery PJ, Marsh GA, Lew AM *et al*. Antiviral activity of arbidol, a broad-spectrum drug for use against respiratory viruses, varies according to test conditions. *J Med Virol* 2012;84:170–181.
26. Cho MW, Ehrenfeld E. Rapid completion of the replication cycle of hepatitis A virus subsequent to reversal of guanidine inhibition. *Virology* 1991;180:770–780.
27. Barton DJ, Black EP, Flanegan JB. Complete replication of poliovirus *in vitro*: preinitiation RNA replication complexes require soluble cellular factors for the synthesis of VPg-linked RNA. *J Virol* 1995;69:5516–5527.
28. Barton DJ, Flanegan JB. Synchronous replication of poliovirus RNA: initiation of negative-strand RNA synthesis requires the guanidine-inhibited activity of protein 2C. *J Virol* 1997;71:8482–8489.
29. Belsham GJ, Normann P. Dynamics of picornavirus RNA replication within infected cells. *J Gen Virol* 2008;89:485–493.
30. Kadam RU, Wilson IA. Structural basis of influenza virus fusion inhibition by the antiviral drug arbidol. *Proc Natl Acad Sci USA* 2017;114:206–214.
31. Martínez-Salas E, Francisco-Velilla R, Fernandez-Chamorro J, Lozano G, Diaz-Toledano R. Picornavirus IRES elements: RNA structure and host protein interactions. *Virus Res* 2015;206:62–73.
32. Daijogo S, Semler BL. Mechanistic intersections between picornavirus translation and RNA replication. *Adv Virus Res* 2011;80:1–24.
33. Stewart H, Walter C, Jones D, Lyons S, Simmonds P *et al*. The non-primate hepacivirus 5' untranslated region possesses internal ribosomal entry site activity. *J Gen Virol* 2013;94:2657–2663.
34. Licursi M, Christian SL, Pongnopparat T, Hirasawa K. *In vitro* and *in vivo* comparison of viral and cellular internal ribosome entry sites for bicistronic vector expression. *Gene Ther* 2011;18:631–636.

35. Loundras EA, Herod MR, Harris M, Stonehouse NJ. Foot-and-mouth disease virus genome replication is unaffected by inhibition of type III phosphatidylinositol-4-kinases. *J Gen Virol* 2016;97:2221–2230.
36. Gunnery S, Mäivali U, Mathews MB. Translation of an uncapped mRNA involves scanning. *J Biol Chem* 1997;272:21642–21646.
37. Belov GA. Dynamic lipid landscape of picornavirus replication organelles. *Curr Opin Virol* 2016;19:1–6.
38. Gorbalenya AE, Koonin EV, Donchenko AP, Blinov VM. A conserved NTP-motif in putative helicases. *Nature* 1988;333:22.
39. Bienz K, Egger D, Troxler M, Pasamontes L. Structural organization of poliovirus RNA replication is mediated by viral proteins of the P2 genomic region. *J Virol* 1990;64:1156–1163.
40. Pincus SE, Diamond DC, Emini EA, Wimmer E. Guanidine-selected mutants of poliovirus: mapping of point mutations to polypeptide 2C. *J Virol* 1986;57:638–646.
41. Egger D, Bienz K. Intracellular location and translocation of silent and active poliovirus replication complexes. *J Gen Virol* 2005;86:707–718.
42. Bienz K, Egger D, Rasser Y, Bossart W. Kinetics and location of poliovirus macromolecular synthesis in correlation to virus-induced cytopathology. *Virology* 1980;100:390–399.
43. Brooks MJ, Sasadeusz JJ, Tannock GA. Antiviral chemotherapeutic agents against respiratory viruses: where are we now and what's in the pipeline? *Curr Opin Pulm Med* 2004;10:197–203.
44. Zhong J, Gastaminza P, Cheng G, Kapadia S, Kato T *et al*. Robust hepatitis C virus infection *in vitro*. *Proc Natl Acad Sci USA* 2005;102:9294–9299.
45. Nakabayashi H, Taketa K, Yamane T, Miyazaki M, Miyano K *et al*. Phenotypical stability of a human hepatoma cell line, HuH-7, in long-term culture with chemically defined medium. *Gan* 1984;75:151–158.
46. Simizu B, Rhim JS, Wiebenga NH. Characterization of the Tacaribe group of arboviruses. 1. propagation and plaque assay of Tacaribe virus in a line of African green monkey kidney cells (Vero). *Exp Biol Med* 1967;125:119–123.
47. Macpherson I, Stoker M. Polyoma transformation of hamster cell clones—an investigation of genetic factors affecting cell competence. *Virology* 1962;16:147–151.
48. Polyak SJ, Morishima C, Lohmann V, Pal S, Lee DY *et al*. Identification of hepatoprotective flavonolignans from silymarin. *Proc Natl Acad Sci USA* 2010;107:5995–5999.
49. Herod MR, Gold S, Lasecka-Dykes L, Wright C, Ward JC *et al*. Genetic economy in picornaviruses: foot-and-mouth disease virus replication exploits alternative precursor cleavage pathways. *PLoS Pathog* 2017;13:e1006666.
50. Herod MR, Ferrer-Orta C, Loundras EA, Ward JC, Verdaguer N *et al*. Both cis and trans activities of foot-and-mouth disease virus 3D polymerase are essential for viral RNA replication. *J Virol* 2016;90:6864–6883.
51. Tuthill TJ, Harlos K, Walter TS, Knowles NJ, Groppelli E *et al*. Equine rhinitis A virus and its low pH empty particle: clues towards an aphthovirus entry mechanism? *PLoS Pathog* 2009;5:e1000620.
52. Baer A, Kehn-Hall K. Viral concentration determination through plaque assays: using traditional and novel overlay systems. *J Vis Exp* 2014;93:e52065.
53. Lindenbach BD. Measuring HCV infectivity produced in cell culture and *in vivo*. *Methods Mol Biol* 2009;510:329–336.